NUMERICAL AND EXPERIMENTAL ANALYSIS OF CRACKED CYLINDRICAL BARS

M.A. Astiz, M. Elices & A. Valiente*

A numerical and experimental research has been performed on cracked cylindrical bars to ascertain the validity of some fracture criteria in three dimensional problems. Numerical results are obtained by means of the finite element method combined with the virtual crack extension method and a new crack tip singular element. Experimental results are checked against CTS and SRS results from the same material.

INTRODUCTION

Cylindrical shapes are very frequent in engineering practice: reinforcing and prestressing bars, shafts, rods. In most of the cases these structural elements are potentially subjected to either fatigue or stress corrosion or corrosion-fatigue problems. These problems are initiated at a surface defect which grows and becomes a surface crack.

At the present stage many uncertainties still exist with respect to cracked bars. A precise calculation of the stress intensity factor has not been achieved. Moreover as this is a three dimensional case some doubts still exist on the fracture criterion which best describes the strength of such elements and its relation to the standard fracture toughness of the material.

The present paper deals with both aspects of the problem.

* Dept. of Physics of Materials
E.T.S.I. Caminos
Ciudad Universitaria
28040-MADRID, ESPAÑA.

A numerical analysis will be presented to compute stress intensity factors in cylindrical bars with semi-elliptical surface cracks. Then an experimental program will be described. This program includes testing of cylindrical bars, CT and SR specimens. Finally results are interpreted and compared to draw some conclusions about fracture criteria to be applied to three-dimensional problems.

NUMERICAL ANALYSIS

The specimen to be analyzed is plotted on Figure 1. Although many mathematical equations could be derived to describe actual fatigue and corrosion crack shapes (see for instance Athanassiadis et al. (1)), a semi-elliptical model crack seems to be the most obvious choice. This specimen is subjected to a uniformly distributed tensile force at both ends. Its length has been taken as 4 times its diameter as a reasonable value to be able to suppose that the singular stress field is negligible at the ends of the specimen.

Stress analysis has been done by means of the finite element method. Eight node brick elements have been used throughout except at the crack border. Around the crack a singular prismatic element has been used as derived by one of the authors (2). This element is a six node triangular prism and represents an extension of Tracey's element (3) which includes two incompatible displacement modes. To improve convergence characteristics further incompatible displacement modes have to be added to the remaining brick elements of the mesh as described by Taylor et al. (4).

As this problem has two planes of symmetry only one fourth of the specimen was considered in the model. The mesh includes 325 nodes and 216 elements. The number of degrees of freedom is 975 although as many as 1860 are eliminated at the element level since they are internal degrees of freedom. This explains why results are good in spite of a relatively coarse mesh.

Stress intensity factor is computed along the crack border by means of the virtual crack extension method as derived by Parks (5) and Hellen (6). The accuracy of this method is greatly increased by combining it with singular elements as pointed out by Hellen (6). As virtual crack extension method gives the energy release rate, G, the stress intensity factor is derived by supposing that a plane strain state holds in the neighbourhood of the crack. This hypothesis has been justified theoretically by Bui (7) although the size of its domain of validity may be limited to a very small zone near the crack as it has been shown by the authors (8).

A wide variety of crack dimensions has been analyzed. The values of the ellipse semi-axes which have been considered are:

$\frac{a}{D}$ = 0.057; 0.100; 0.143; 0.200; 0.257; 0.314; 0.371; 0.429; 0.486

$\frac{a}{c}$ = 0.0; 0.2; 0.5; 1.0; 2.0

Then 45 cases were analyzed. The accuracy of the results may be checked by comparing them to existing data for the straight crack (a/c = 0). This problem has been studied by many authors but we have selected for comparison the results which have been obtained by methods different from the finite element method: boundary element method (1), three dimensional photoelasticity (9) and two dimensional experimental compliance measurement by Bush (10). Results are represented on Fig. 2 in terms of the non dimensional coefficient M (= $K_I/\sigma\sqrt{\pi a}$) evaluated at the center of the crack. A very good agreement with (1) has been obtained and also the agreement with experimental results (9, 10) is fair.

Design charts for the stress intensity factor at the center of the crack are presented on Fig. 3 as a function of crack dimensions.

EXPERIMENTAL PROGRAM

It is well known that the fracture criterion based on a critical value of the stress intensity factor K_I is a consequence of the similarity principle for plane problems. For three-dimensional cases K_I varies along the crack front and this criterion must be generalized. Another important question to be considered is the role that the standard fracture toughness, K_{IC}, plays in the new criterion.

As the objective of this research is to ascertain the validity of a given fracture criterion for cracked bars under linear elastic behaviour all the tests have been performed at a cryogenic temperature, namely at liquid nitrogen temperature (-196ºC). Specimens have been cut from a reinforcing bar (diameter 58 mm). The mechanical characteristics of this material at ambient temperature and at liquid nitrogen temperature are specified in table 1. Corresponding stress strain curves are plotted on Fig. 4.

TABLE 1 - Material Mechanical Properties

Material Property	20ºC	-196ºC
Young's Modulus (MPa)	218000	220000
0.2% Yield Stress (MPa)	550	900
U.T.S. (MPa)	790	>1090

Three different types of specimens have been prepared: cylindrical bars, CT and SR (Short Rod) specimens. The relative position of the fracture test specimens in the reinforcing bar has been chosen such that the orientation of the cracks is the same to avoid side effects due to possible anisotropic properties of the original reinforcing bar (see Fig. 5). Three, 20 mm thick, CT specimens and five SR specimens (diameter 12.7 mm) have been tested. The number of cylindrical bars has been larger: eight specimens with diameters 5, 7, 10 and 16.7 mm. The reason for choosing four different diameter values consists in trying to know the influence of this parameter on fracture results.

CT and cylindrical bar specimens were precracked by fatigue at ambient temperature. Cooling is performed by immersion in liquid nitrogen. Fracture tests are made on a static machine and by maintaining the specimens inside liquid nitrogen during the whole test. The testing arrangement is described on Figure 6.

Results are summarized on tables 2-4 along with the corresponding K_Q values for the center of the crack border.

TABLE 2 - CTS Tests Results at -196ºC.

B(mm)	W(mm)	a/w	K_Q(MPa $m^{1/2}$)
20.40	40.15	0.531	33.2
20.40	40.00	0.536	34.9
20.30	40.15	0.538	33.1

TABLE 3 - SRS Tests Results at -196ºC.

B(mm)	K_Q(MPa $m^{1/2}$)
12.70	31.7
12.70	32.0
12.70	32.1
12.70	31.7
12.70	30.3

TABLE 4 - Cracked Cylindrical Bars Results at -196ºC.

D(mm)	a/D	a/c	K_Q(MPa $m^{1/2}$)
16.7	0.222	0.55	29.9
16.7	0.341	0.56	35.2
10.0	0.250	0.61	31.2
10.0	0.366	0.58	32.7
10.0	0.412	0.51	35.4
7.0	0.296	0.68	33.6
7.0	0.380	0.41	32.5
5.0	0.326	0.64	33.3

ANALYSIS OF THE RESULTS

By looking at tables 2-4 it may be noted that K_Q values are very similar in all three cases. In fact the comparison may be done in terms of mean values and relative standard deviations:

CTS: $\overline{K}_Q$ = 33.7 MPa $m^{1/2}$

δ = 3.0%

SRS: $\overline{K}_Q = 31.6$ MPa $m^{1/2}$

$\delta = 2.3\%$

CCB: $\overline{K}_Q = 33.0$ MPa $m^{1/2}$

$\delta = 5.6\%$

Mean values are close to each other and by looking at standard deviations it is very difficult to affirm that one of them is significantly different from the others. On the other side standard deviations demonstrate that CTS and SRS are standard tests with very strict limitations on crack shape and dimensions whereas relative crack depth on cylindrical specimens varies between 0.222 and 0.412.

Diameter influence is not apparent from these results because of high dispersion. By analyzing mean K_Q values for each diameter value one may notice a slight toughness decrease for increasing diameters but this is not significant.

Another fact may be noticed from these results. As CTS tests have been performed in full agreement with the ASTM Standard Specification, corresponding K_Q value is the material fracture toughness, K_{IC}. Then, if we consider this value as a reference, the error in SRS results is 6% while the error in cylindrical bars results is only 2%. This fact indicates that, after some standardization, the cylindrical bar test may be at least as good as the short rod test. Nevertheless one has to keep in mind that these results were obtained at a cryogenic temperature, for brittle materials. When crack tip plasticity is present relative merits of each one of the tests which have been considered may change dramatically.

Finally the last point to investigate is the validity of the fracture criterion. The criterion which has been used here is a generalization of Irwin's criterion: fracture will occur when the maximum value of the stress intensity factor along the crack front attains a critical value. This criterion can be described by the equation,

$$\text{Max } K_I(s) = K_{IC} \qquad (1)$$

where s is the arc length measured along the crack front. D'Escatha and Labbens (11) have shown that this criterion is equivalent to the generalized Griffith criterion which consists in obtaining the maximum energy release rate for any crack extension and making it equal to the critical value $K_{IC}^2(1-\nu^2)/E$.

In our case the crack dimension have been checked to be such that the stress intensity factor is maximum at the center

of the crack for all the specimens. Then, as K_Q has been computed at the center of the crack, equation (1) has been found to be valid for a brittle material with the uncertainties due to the small number of specimens and the dispersion of the results.

Bui and Dang Van (12) have proposed a more general fracture criterion for three dimensional cracked bodies in which they take into account not only the energy necessary to create new cracked area, but also the energies necessary to elongate and to bend the crack edge. Then the energy dissipation rate depends on the curvature radius of the crack front. This criterion is not equivalent to the generalized Irwin criterion (1) and we should find significant differences on G_Q values for different diameters and crack shapes. For this reason we have explored if it is posible to detect some kind of dependence of G_Q on the curvature radius of the crack. The graphical representation of G_Q values as a function of curvature radius (Fig. 7) at the center of the crack suggests a correlation between both variables. This is a very important fact if we take into account that the crack tip plastic zone must be extremely small in this case. Then more tests and at different temperatures should be undertaken to ascertain the validity of the Bui and Van fracture criterion. At the present stage a linear interpolation of G_Q as a function of $1/\rho$ would give a very low value of K_{IC} (namely 22 MPa $m^{1/2}$) as compared to CTS results. A parabolic interpolation as recomended by Bui and Van would give better results but it cannot be done on the basis of a small number of tests.

CONCLUSIONS

The main conclusions which arise from this work relate to the use of fracture criteria in three dimensional problems. The generalized Irwin criterion has been found to be adequate for this particular case. Nevertheless more research has to be undertaken on the Bui and Van criterion to check its validity.

AKNOWLEDGEMENTS

This work has been sponsored by the Spanish Commission for Scientific and Technological Research (CAICYT) under grant number 0511-84.

REFERENCES

(1) Athanassiadis, A., Boissenot, J.M., Brevet, P. François, D., Int. J. of Fracture, Vol. 17, 1981, pp. 553-566.

(2) Astiz, M.A., Int. J. of Fracture, (to be published).

(3) Tracey, D.M., Nuclear Eng. and Design, Vol. 26, 1974, pp. 282-290.

(4) Taylor, R.L., Beresford, P.J., Wilson, E.L., Int. J. of Numerical Methods in Engineering, Vol. 10, 1976, pp. 1211--1220.

(5) Parks, D.M., Int. J. of Fracture, Vol. 10, 1974, pp. 487-502.

(6) Hellen, T.K., Int. J. of Numerical Methods in Engineering, Vol. 9, 1975, pp. 187-207.

(7) Bui, H.D., J. of the Mechanics and Physics of Solids, Vol. 26, 1978, pp. 29-39.

(8) Astiz, M.A., Elices, M., Valiente, A., Anales de Física, Vol. B79, 1983, pp. 65-76.

(9) Astiz, M.A., Elices, M., Morton, J., Valiente, A., Proc. of the Soc. for Experimental Stress Analysis, Dearbon, 1981.

(10) Bush, A.J., J. of Testing and Evaluation, Vol. 9, 1981, pp. 216-223.

(11) D'Escatha, Y., Labbens, R., J. de Mécanique Appliquée, Vol. 2, pp. 541-552.

(12) Bui, H.D., Dang Van, K., J. de Mécanique Appliquée, Vol. 3, pp. 205-225.

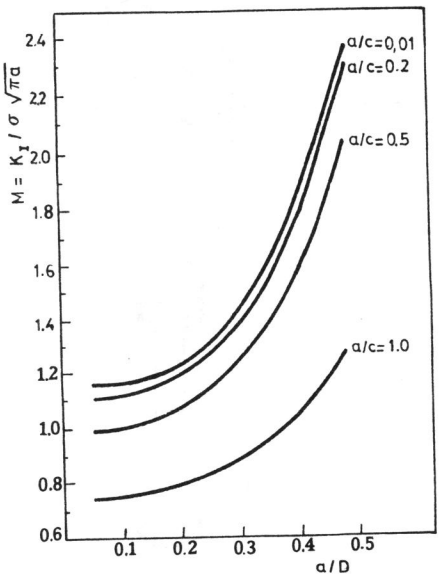

Figure 3 Design chart for K_I.

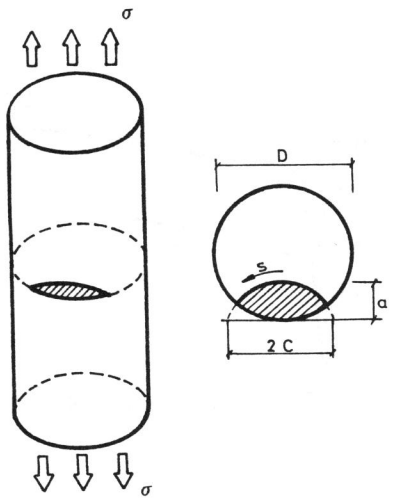

Figure 1 Geometric description.

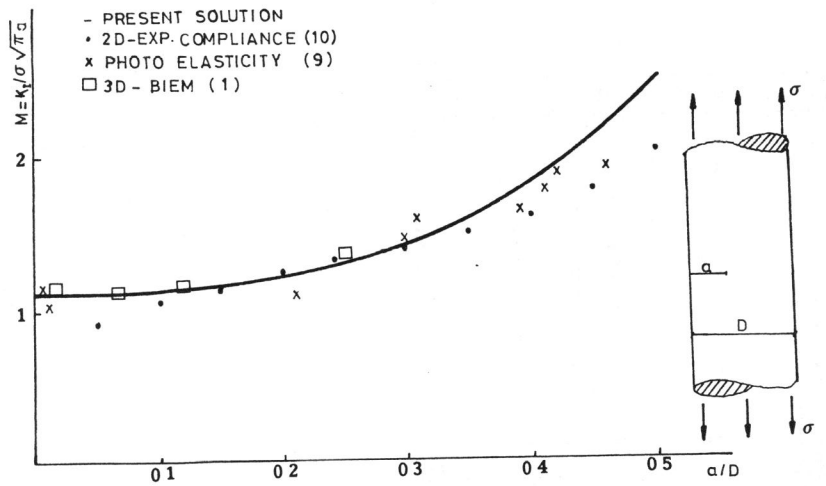

Figure 2 K_I values for a straight edge crack.

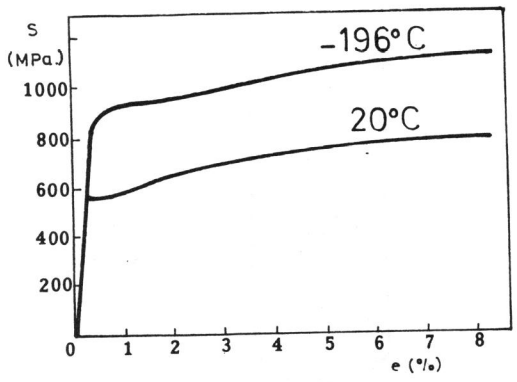

Figure 4 Stress strain curves.

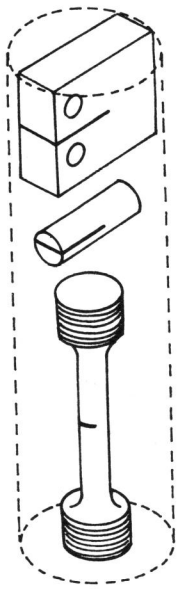

Figure 5 Relative position of the specimens.

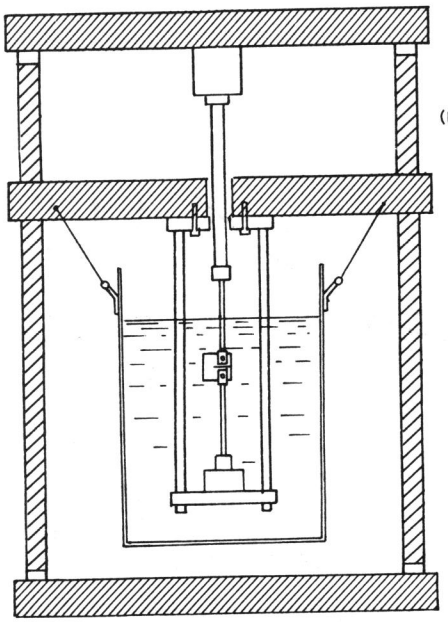

Figure 6 Testing arrangement.

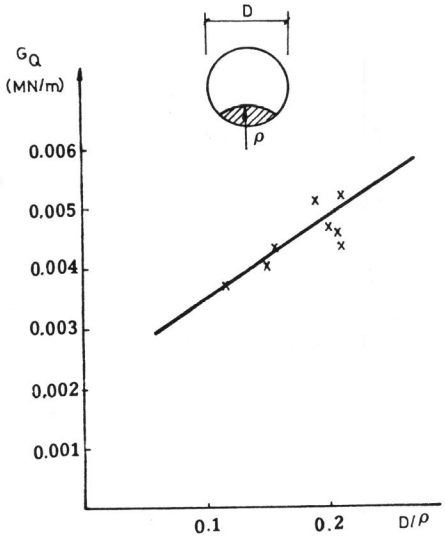

Figure 7 Influence of the curvature radius.